Russian Meteorology and Hydrology
No. 12, pp. 1–8, 2004

Meteorologiya i Gidrologiya
UDC [551.513+551.465].001.572:551.526.6(265-062.5)

EL NIÑO IN A COUPLED OCEAN–ATMOSPHERE GENERAL CIRCULATION MODEL

E. M. Volodin* and N. A. Dianskii*

The interannual variability of equatorial Pacific sea surface temperature (SST) is simulated in an 80-year experiment with the INM RAS coupled ocean-atmosphere general circulation model. The model correctly reproduces the observed spectral peak of variability at 3–5 years and observed features of negative SST anomalies in comparison with positive ones. However, the SST variability maximum in the El Niño region is shifted in the model to the west compared with the observational data. A possible cause is the overestimation of the mean velocity of upwelling in the central and western Pacific. The improved simulation of the El Niño statistics compared with the original version of the model is achieved by changing a parametrization of low cloud, deep convection, and dynamics in the atmospheric block and by using a C grid instead of a B grid in the ocean model.

INTRODUCTION

The interannual variability of equatorial Pacific SST and associated El Niño and La Niña events are among the strongest signals of natural climate variability. Many studies are aimed at determining the mechanisms of this variability and its numerical simulation.

Modern coupled ocean–atmosphere general circulation models (OAGCM) can reproduce many features of the observed interannual variability in the tropical Pacific. The El Niño in a modern coupled OAGCM is best reproduced in [5], where the equatorial Pacific SST variability is analyzed using 14 coupled models participating in the CMIP project [5]. According to the results from more than half of the models considered, the mean amplitude of El Niño is nearly equal to or slightly less than the observed one. Other models substantially underestimate the amplitude of the equatorial Pacific SST variability. The main disadvantages of most models [5] are the following. The models with no heat flux correction underestimate the difference in SST between the eastern and western tropical Pacific. This is probably related to the underestimated velocity of upwelling near the South American coast and its overestimation in the central Pacific. The latter explains the shift to the west (compared with the observational data) of the area of the maximum SST variability. In addition, according to the data from many models, the characteristic period of the El Niño is 2–3 years, while according to the observational data it is 3–5 years. No distinct relation between the quality of the reproduced El Niño and model characteristics, for example, horizontal and vertical resolution or inclusion of any physical parametrizations, has been established. The conclusions of [5] are basically confirmed by the recent works on modeling El Niño using OAGCM [9, 10, 15, 16].

* Institute of Numerical Mathematics, Russian Academy of Sciences

The El Niño in a coupled ocean–atmosphere model of the Institute of Numerical Mathematics, Russian Academy of Sciences (INM RAS), is briefly described in [4]. The model correctly reproduced the position of the region of the maximum SST variability. Compared with the observational data, the amplitude of variability is slightly underestimated. The main disadvantage of the model is that the model magnitude of negative equatorial Pacific SST anomalies is much greater than that of positive ones, while in nature the situation is quite opposite: the SST anomalies during El Niño are on average somewhat greater than during La Niña. This work is dealing with the improved statistics of El Niño in a new version of the INM RAS model.

DESCRIPTION OF THE MODEL AND NUMERICAL EXPERIMENTS

The OAGCM is described in detail in [4]. The resolution in the atmospheric block is 5° in longitude, 4° in latitude, and 21 levels in the vertical in sigma coordinates. Hydrothermodynamic equations are solved on a C grid. Parametrizations of radiation [2], deep and shallow convection [7], soil and land surface processes [1], and gravity wave drag [8, 13] are used. The ocean model resolution is $2.5 \times 2°$ in longitude and latitude and 33 sigma levels in the vertical. Turbulence is parametrized in accordance with [12]. In coupling the atmosphere and ocean models, the flux correction is not used. The coupled model assumes the observed monthly mean climatic ice distribution because the version of the model with interactive ice was still under development at the time the paper was prepared. In the original version of the coupled model [4], the Arakawa B grid is used for discretization of the ocean dynamic equations in the horizontal plane.

In the new version of the ocean model, for discretization of the dynamic equations, the C grid was used, which has lower dissipativeness, which made it possible to introduce a free-slip condition instead of adhesion on lateral boundaries and to reduce horizontal diffusivity. The use of the C grid made it possible to more adequately approximate the numerical domain in the straits. For example, the ocean model used in the coupled OAGCM provided a more precise description of the salt exchange between the Atlantic and the Mediterranean Sea through Gibraltar, which is very important for describing the thermohaline circulation in the North Atlantic. The main difference in the numerical implementation between the previous version of the ocean model on the B grid and the new version on the C grid is that the difference approximation for the stream function in the new version was carried out at the difference level. The equation for the stream function on the C grid is constructed by means of difference cross-differentiation of the equations for the depth-averaged zonal and meridional velocity components which are written at corresponding points not coinciding on the C grid. The original skew-symmetry was preserved.

In the atmospheric block of the model, the tuning of parametrization of low-level clouds was changed. In the original version, the cloud amount C is a linear function of relative humidity r:

$$C = \alpha + \beta r,$$

where α and β depend on temperature, altitude, type of surface (land or ocean), and temperature lapse rate. The dependence on the temperature lapse rate is such that below the inversion layer the cloud amount is greater than that at the same relative humidity in a less stable stratification. In the new version of the model, this dependence of the cloud amount on stratification is weak. In addition, in the atmospheric block of the model, instead of the finite-difference scheme [6] where the equations are written in Gromek–Lamb form, the scheme described in [3] is used, with the equations written in advective form. That made it possible to provide a more correct description of high spatial harmonics and to introduce horizontal viscosity and diffusion of the eighth order instead of those of the fourth order used in the original version of the model. Changes have also been introduced into parametrization of deep convection.

The new version of the model was used to perform a numerical experiment on modern climate simulation that was similar to the experiment with the original version [4]. For initial data for the experiment in the atmosphere, we used the state determined from the integration of the atmospheric block with a given

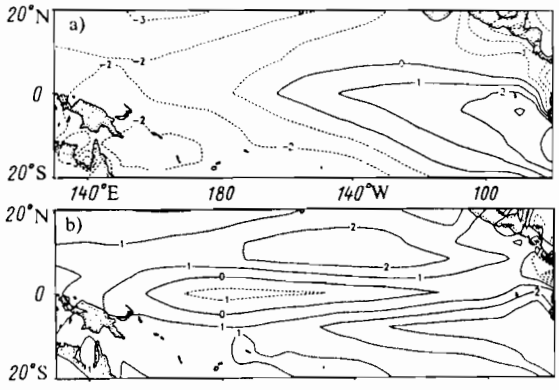

Fig. 1. The error of the reproduced annual mean SST in the tropical Pacific from (a) the original model and (b) the new model. Contour interval is 1 K. Data from [14] are used as observations.

observed annual SST variation, and in the ocean, the observed temperature and salinity distribution [11] and zero velocities were used. The model climate reached a steady state in 50 years, and the data of the subsequent 80 years of calculations have been processed and presented in this work. The results of the experiment with the new version of the model are compared with the data from the original version and with the NCEP reanalysis data for 1950–2000 used as observational data.

RESULTS OF NUMERICAL EXPERIMENTS

The annual mean error of simulation of the tropical Pacific SST in the original and new versions of the model is given in Fig. 1. In the original version, the temperature is 1–3 K underestimated in the western region and 1–3 K overestimated near the South American coast and near the equator, in the eastern ocean. This means that the mean velocity of upwelling near the equator and the eastern coast is underestimated. In the new version of the model, the temperature is 1–3 K overestimated almost everywhere, except the equatorial part of the ocean, where the difference from the observed temperature is not greater than 1 K. This means that the mean upwelling velocity in the new version of the model is likely to be overestimated slightly. The intensified east trade winds (when turning to a new scheme of calculation of the atmospheric dynamics) resulted in the intensification of upwelling. As will be seen below, the accuracy of simulation of the average state, mainly the mean velocity of upwelling, influences the simulation of the interannual SST variability.

The time variation of the monthly mean SST anomaly relative to the climatic annual variation in the El Niño region (180–100°W, 4°N–4°S) derived from the observational data and the original and new versions of the model is shown in Fig. 2. In the original version of the model, the SST in the El Niño region slightly exceeds the climatic mean most of the time, but several times during the numerical experiment the temperature decreases sharply for a short time. Maximum positive SST deviations from the climatic mean do not exceed 1 K, while negative anomalies reach 3–4 K. On the whole, during the numerical experiment the temperature exceeds the mean 60% of the time.

At the same time, according to the observational data, the SST exceeds the climatic mean during the period less than half of all the time (45%). Maximum positive SST anomalies, according to the observational data, reach 2.5–3 K, while maximum negative anomalies do not exceed 2 K. This characteristic variability of the SST in the El Niño region is reproduced in the new version of the model. The sea surface temperature exceeds the climatic mean 44% of the time of the whole experiment, while the values of posi-

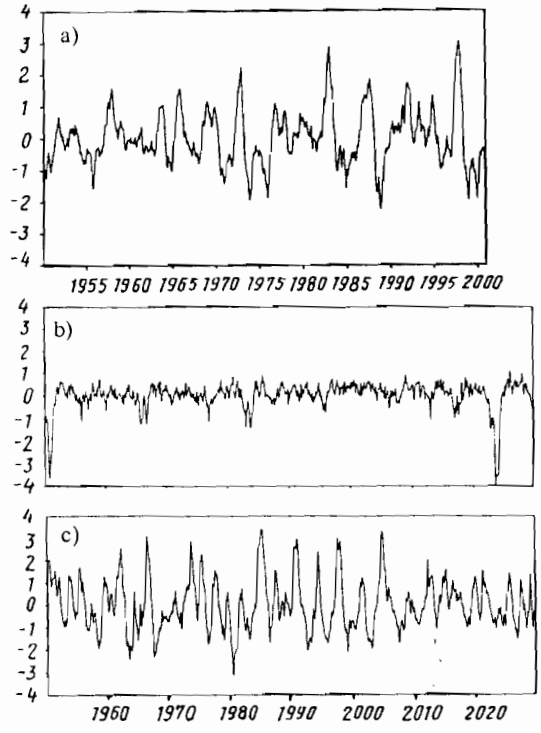

Fig. 2

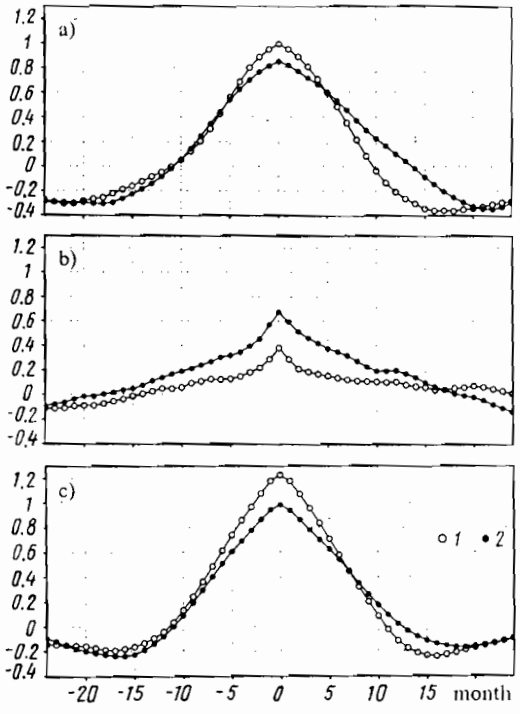

Fig. 3

Fig. 2. Time variation of SST anomalies (K) in the region 180–100°W, 4°N–4°S from (a) 1950–2000 observational data, (b) original version, and (c) new version of the model. For convenience, the time scale chosen for the modeling results is the same as that for the observations.

Fig. 3. Average time variation of SST anomalies (K) during (1) El Niño and (2) La Niña from (a) observations, (b) original version, and (c) new version of the model. Data for La Niña are with the opposite sign. The time lag (month) is plotted on the abscissa.

tive SST maximum are greater in magnitude than those of negative ones. This difference from the original version of the model is due mainly to the change in parametrization of the low sub-inversion clouds. The prevailing small positive SST anomalies in the El Niño region and individual obviously manifested SST minimums are connected with the wrong simulation of the interaction between SST and low-level clouds in the model. Most of the time, during weak positive SST anomalies, the surface inversion and the corresponding low-level clouds in the El Niño region are absent. However, as the upwelling velocity increases and SST decreases slightly, the inversion conditions are formed and the sub-inversion cloud amount increases sharply. This results in a substantial reduction of the incoming short-wave radiation and an even greater SST drop. At the same time, in the real atmosphere the amount of the sub-inversion clouds over the equatorial Pacific appears to be not very large even during negative SST anomalies, since the temperature lapse rate there is always close to the moist-adiabatic one. In the new version of the model, the dependence of the amount of sub-inversion clouds on vertical stratification is weak, which resulted in a weaker positive feedback: SST fall–cloud amount increase–further SST fall. As a result, the amount of sub-inversion clouds over the equatorial Pacific decreased strongly, the negative anomalies in the El Niño region also decreased, while the positive ones increased, which agrees with the observational data.

The differences between the time variation of the SST anomalies for El Niño and La Niña events derived from the observational data and the model are clearly seen in Fig. 3. The El Niño case is the case where the monthly mean SST in the El Niño region exceeds the climatic mean by 0.5 SD of that month. In this figure, the SST anomaly averaged over all El Niño months corresponds to the zero time lag. The

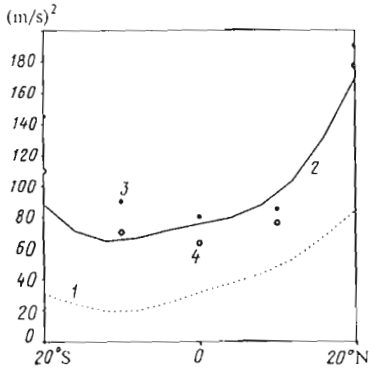

Fig. 4

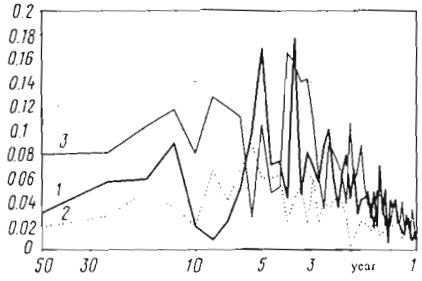

Fig. 5

Fig. 4. Distribution of kinetic energy in the tropical atmosphere at 200 hPa in December–February from (1) original and (2) new versions of the model and (3) ECMWF and (4) NCEP reanalysis data.

Fig. 5. Temporal spectrum of SST anomalies (K) in the El Niño region from (1) observations, (2) original version, and (3) new version of the model. The *x*-coordinate is the period in years.

SST anomaly averaged over all cases N months after El Niño corresponds to a positive lag of N months. To a negative lag of N months there corresponds an SST anomaly averaged over all cases N months before the El Niño months. Similarly, the La Niña case is the case where SST is 0.5 SD below the climatic mean of that month. The SST data for La Niña are given with the opposite sign.

From the observational data in Fig. 3, it follows that the mean SST anomaly during El Niño is 1 K, and 0.8 K during La Niña. However, during the months after El Niño the SST anomaly drops much faster than during the months after La Niña. For example, 12 months after El Niño, the SST anomaly, on average, changes the sign and amounts to about –0.2 K, while 12 months after La Niña the SST anomaly, on average, does not change its sign. These differences between El Niño and La Niña are well reproduced in the new version of the model. And, on the contrary, in the original version the mean SST anomaly during El Niño is only 0.4 K, and about 0.7 K during La Niña.

The amplitude of variability in the El Niño region increased due to the increased internal variability of the tropical atmosphere. It was a result of a readjustment of parametrization of deep convection. The model uses the parametrization of convection [7], where in the case of moist instability the vertical temperature and humidity profiles approach some reference profiles. In the new version of the model, these profiles were chosen such that most of the heat was released in the middle troposphere, which agrees better with available observational estimates. As a result, the variability of atmospheric dynamics in the tropics increased. In particular, the amplitude of 30–60 day oscillations, underestimated in the original model, became close to the observational data in the new model. Figure 4 shows the distribution of the kinetic energy in the tropical atmosphere at 200 hPa from the original and the new version of the model and from the NCEP and ECMWF reanalysis data. In the original version, the variability energy is 2–4 times lower than that in the reanalysis, while in the new version of the model it is close to the reanalysis data.

In the observed spectrum of the SST variability in the El Niño region, the peaks at periods of about 3.5 and 5 years are most pronounced (Fig. 5). There is a variability maximum with a period of 10–15 years. In the new version of the model, the most pronounced peak is at periods of 3.5–4 years, less pronounced peaks are observed at periods of 5 and 8–12 years. On the whole, the new version of the model provides a correct amplitude of oscillations with periods of 3–5 years and overestimates the amplitude of variability of longer periods. In the old version of the model, the most pronounced spectral peak of the

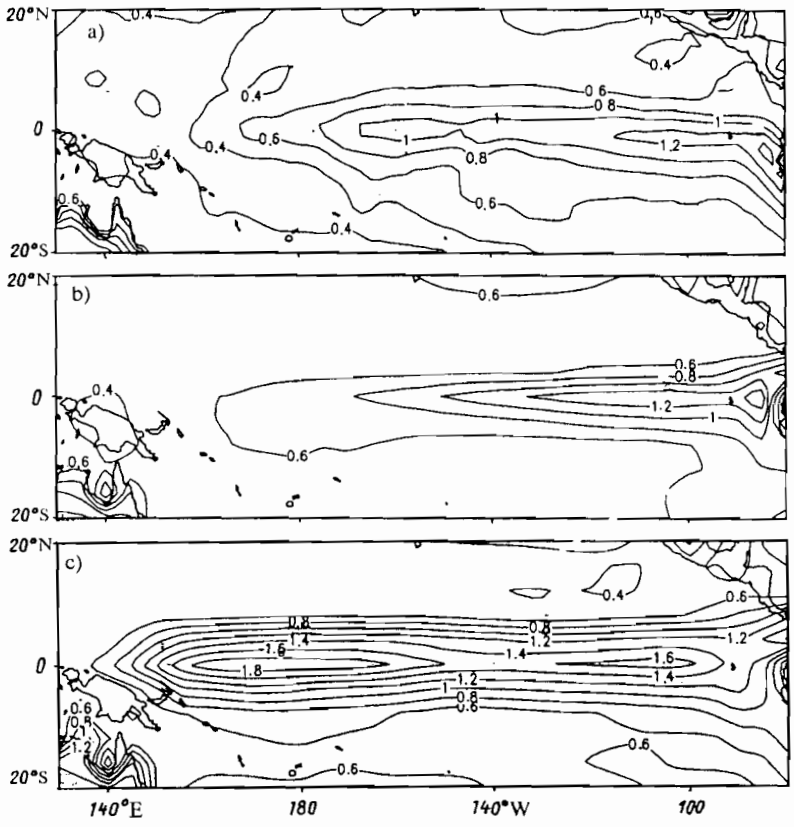

Fig. 6. Standard deviation of monthly mean SST from (a) observations, (b) original version, and (c) new version of the model. Control interval is 0.2 K.

SST variability in the El Niño region corresponds to a period of 7 years, and its magnitude is approximately two times less than the magnitude of a maximum peak according to the observational data. A more correct simulation of the spectrum of the SST variability in the El Niño region, including the increased magnitude of the spectral peaks, is achieved mainly by tuning the parametrization of deep convection and changing of horizontal diffusion in the atmospheric block of the model.

At the same time, the geographical distribution of SST variability in the Pacific is worse in the new version than in the original one. According to the observational data, the amplitude of variability is maximal in the eastern equatorial Pacific, near the South American coasts, where SD of the SST reaches 1.2–1.4 K (Fig. 6). In the western Pacific, according to the observational data, the SD does not exceed 0.4–0.6 K. This feature is well simulated in the old version of the model. In the new model, the maximum of variability is located along the equator not only in the eastern but also in the central and western Pacific, which agrees less with the actual data. This error in the new model is probably connected with the reproduced average state. In the new version, the climatic mean SST at the equator in the central and western Pacific is underestimated (Fig. 1), which is indicative of the overestimated velocity of upwelling. The breakdown of trade winds over the Pacific leads in the new model to disturbances in upwelling and positive SST anomaly not only in the eastern but also in the central and western equatorial Pacific. In the old version of the model, the upwelling in the central Pacific is weaker than in the observational data, and this results in a small SD of the SST in the central and western Pacific.

Finally, let us consider the remote response of the atmospheric circulation to the SST anomaly in the equatorial Pacific in the new version of the model. Figure 7 shows the average difference of sea-level pressure during El Niño and La Niña months from the observations and the new version of the model.

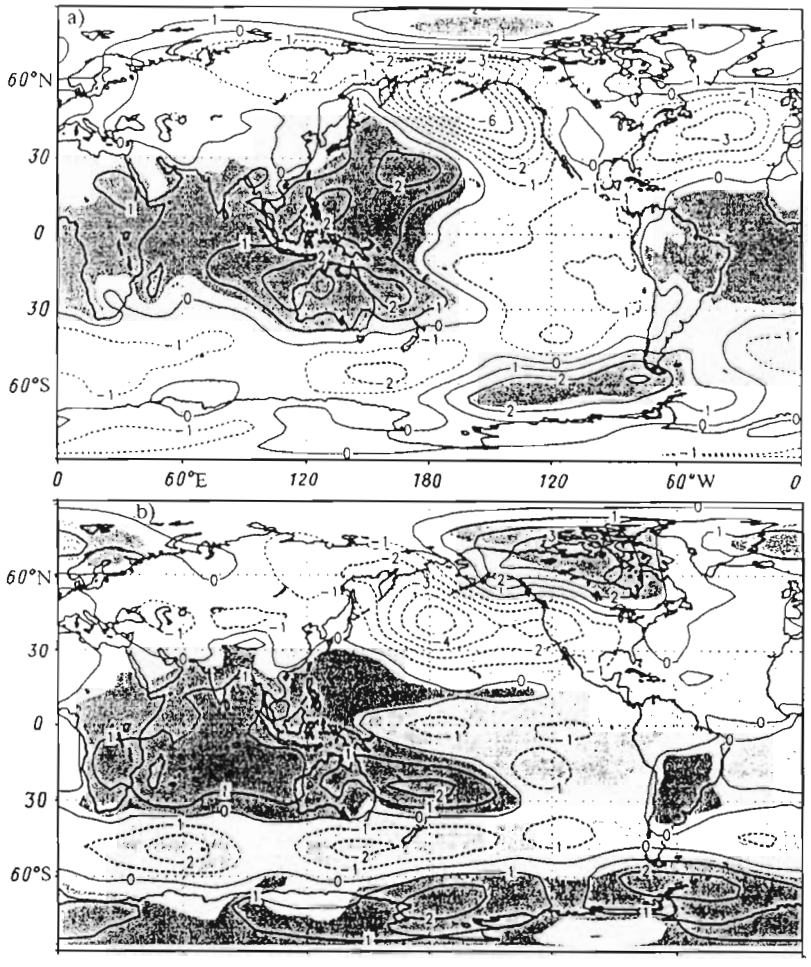

Fig. 7. Sea-level pressure difference between El Niño and La Niña months from (a) observations and (b) the new version of the model. Data are for December, January, and February. Dark areas correspond to statistical significance of the difference in accordance with the Student *t*-test with probability 0.95. Contour interval is 1 hPa.

The data for December–February are presented. In the tropics during El Niño, the pressure decreases by 1 hPa over the central and eastern Pacific and increases by 1–2 hPa in the western Pacific, over the Indian Ocean, Australia, and Africa. These changes are well reproduced in the model. In midlatitudes, the largest response is observed over the northern Pacific, where the pressure drops by 2–6 hPa. The model data are close to the observational data. The differences between the model and observational data are observed over northern Canada and over the Atlantic east of the United States. They can be attributed to the fact that the El Niño in the model occurs just west of the place in the observational data. Probably, a special paper will be devoted to a more detailed analysis of the response of the atmospheric circulation to El Niño.

CONCLUSIONS

The interannual sea surface temperature (SST) variability in the tropical Pacific in the new version of the INM RAS coupled ocean–atmosphere general circulation model is considered. The model adequately provides the observed statistics of El Niño and La-Niña, including characteristic SST anomalies, temporal spectrum, and the difference in the atmospheric circulation between El Niño and La Niña years. The improved reproduction of these phenomena compared with the original version of the model was the result

of the adjustment of parametrization of low clouds, deep convection, a modified scheme of the dynamic block, and the use of a C grid for solution of equations of the ocean dynamics. The main drawback of the new model in the simulation of El Niño is a westward shift of the region of the maximum SST variability. Obviously, it is due to a very high velocity of upwelling in the central Pacific. Such a drawback is characteristic of many modern ocean–atmosphere general circulation models. Possibly, this drawback can be overcome by increasing horizontal resolution in the oceanic block of the model, at least near the equator.

The work was supported by the Russian Foundation for Basic Research (grants 03-05-64358 and 02-05-64909) and Ministry of Science and Technologies RF (grant NSh-1958-2003-5).

REFERENCES

[1] E. M. Volodin and V. N. Lykosov, "Parametrization of heat- and moisture exchange processes in the vegetation–soil system for modeling atmospheric general circulation. Part I: Description and calculations using local observational data," Izv. Russ. Acad. Sci., Atmospheric and Oceanic Physics, vol. 34, no. 4, 1998.

[2] V. Ya. Galin, "Parametrization of radiation processes in the INM RAS atmospheric model," Izv. Russ. Acad. Sci., Atmospheric and Oceanic Physics, vol. 34, no. 3, 1998.

[3] V. Ya. Galin, E. M. Volodin, and S. P. Smyshlyaev, "Atmospheric general circulation model of INM RAS with ozone dynamics," Russian Meteorology and Hydrology, no. 5, 2003.

[4] N. A. Dianskii and E. M. Volodin, "Modern climate in the coupled ocean–atmosphere general circulation model," Izv. Russ. Acad. Sci., Atmospheric and Oceanic Physics, vol. 38, no. 6, 2002.

[5] K. Rao Achuta, K. R. Sperber, and the CMIP modeling group, "El Niño/Southern Oscillation in Coupled Models," PCMDI Report no. 6, 2000.

[6] A. Arakawa and V. R. Lamb, "A potential enstrophy and energy conserving scheme for shallow water equations," Mon. Wea. Rev., vol. 109, 1981.

[7] A. K. Betts, "A new convective adjustment scheme. Part I. Observational and theoretical basis," Quart. J. Roy. Meteorol. Soc., vol. 112, 1986.

[8] C. O. Hines, "Doppler spread parametrization of gravity wave momentum deposition in the middle atmosphere. Part 2. Broad and quasimonochromatic spectra, and implementation," J. Atmos. Sol. Terr. Phys., vol. 59, 1997.

[9] E. Guilyardi, P. Delecluse, S. Gualdi, and A. Navarra, "Mechanisms of ENSO phase change in a coupled GCM," J. Climate, vol. 16, 2003.

[10] B. P. Kirtman, Y. Fan, and K. Schnieder, "The COLA global coupled and anomaly coupled ocean–atmosphere GCM," J. Climate, vol. 15, 2002.

[11] S. Levitus, World Ocean Atlas–CDROM data set, US Department of Commerce, National Oceanic and Atmospheric Administration, National Environmental Satellite Data and Information Service, National Oceanographic Data Center, Ocean Climate Laboratory, 1994.

[12] R. C. Pacanovsky and G. Philander, "Parametrization of vertical mixing in numerical models of the tropical ocean," J. Phys. Oceanogr., vol. 11, 1981.

[13] T. N. Palmer, G. J. Shutts, and R. Swinbank, "Alleviation of a systematic westerly bias in general circulation and numerical weather prediction models through an orographic gravity wave drag parametrization," Quart. J. Roy. Meteorol. Soc., vol. 112, 1986.

[14] R. W. Reynolds and T. M. Smith, "Improved global sea surface temperature analysis using optimum interpolation," J. Climate, vol. 70, 1994.

[15] E. K. Schneider, "Understanding differences between the equatorial Pacific as simulated by two coupled GCMs," J. Climate, vol. 15, 2002.

[16] D. J. Vimont, D. S. Battisti, and A. C. Hirst, "Pacific interannual and interdecadal equatorial variability in a 1000-yr simulation of the SSIRO coupled general circulation model," J. Climate, vol. 15, 2002.

20 May 2004